PROPERTIES AND COMPRESSIBILITY OF Fe/SiO_2 COMPOSITE COATED POWDERS

A. Mišková, E. Dudrová, M. Kabátová, J. Harvanová

Abstract

Soft magnetic composites prepared by powder technology consist of magnetically soft particles (usually Fe) which are coated with a suitable electro insulation layer. An important phase of their preparation is shaping without damaging the insulation layer. This contribution deals with the effect of both the size and shape of iron particles and the effect of binder addition (Silane) on the compressibility of composite coated powders Fe/SiO_2 prepared by the sol-gel method with a following calcination at 400°C. At low pressing pressures, the densification of coated powders is controlled by the shape of iron particles (the apparent density is higher for powders with spherical particles), while in the stage of prevalent densification by plastic deformation the compressibility depends on the ability of iron core to plastic deformation without any substantial effect of the SiO_2 coating. The compressibility was quantified by the compression ratio, relative density and parameters of a compaction equation.

Keywords: composite coated powders Fe/SiO_2, compressibility, microstructure

INTRODUCTION

Modern technologies and new powerful devices require new materials with exceptional properties that need specific approaches involving unusual chemical concepts and unconventional technologies. One specific group of materials which needs a spatial "network" microstructure are the soft magnetic composites consisting of magnetically soft particles (usually Fe) coated with a suitable electro insulating layer, such as ceramics or polymer, e.g. [1-3]. The development of these materials is motivated by the objective of replacing the conventional soft magnetic materials, i.e. laminated steel sheets by cheaper powder composite materials with comparable mechanical and electromagnetic properties, e.g. [4]. Currently, this is mainly the conception of modern materials, such as $Fe/FePO_4$ [5,6], Fe/MgO [7,8] and Fe/SiO_2 [9]. Some of them are at the research level, while others are industrially applied, e.g. [10,11]. Considerable attention is also given to materials based on Fe/MgO powders, e.g. [12] because of their higher thermal stability. Less information has been published about SMCs based on the Fe/SiO_2, which are interesting because of their favourable thermal stability and relatively simple material base. A critical step of the production technology is compaction, in which the highest possible density must be achieved without damaging the electro insulating coating. Different methods are used, but the most economically advantageous approach is cold pressing. This contribution focuses on the effect of the iron particle properties (shape and size) and the effect of the addition of Silane as a binder on the compressibility and microstructure of Fe/SiO_2 composite powders prepared by the sol-gel method.

Andrea Mišková, Eva Dudrová, Margita Kabátová, Jarmila Harvanová, Institute of Materials Research, Slovak Academy of Sciences, Košice, Slovak Republic

EXPERIMENTAL PROCEDURE

The starting powder used was commercial water atomised iron powder ASC 100.29 (Höganäs AB) in as received state - with particles of irregular shape, Fig.1a (signed N) and after milling in a mill Pallmann REFL18 at 11,000 rpm thus obtaining particles of a spherical shape, Fig.1b (signed M). Milled powder was annealed at 600°C for 60 min in an atmosphere of N_2+10%H_2. Three sieved fractions with different particle sizes were prepared for testing: <200 μm (for powder N, signed P) or <160 μm (for powder M, signed P), 100-160 μm (signed 1) and 45-63 μm (signed 2), Table 1.

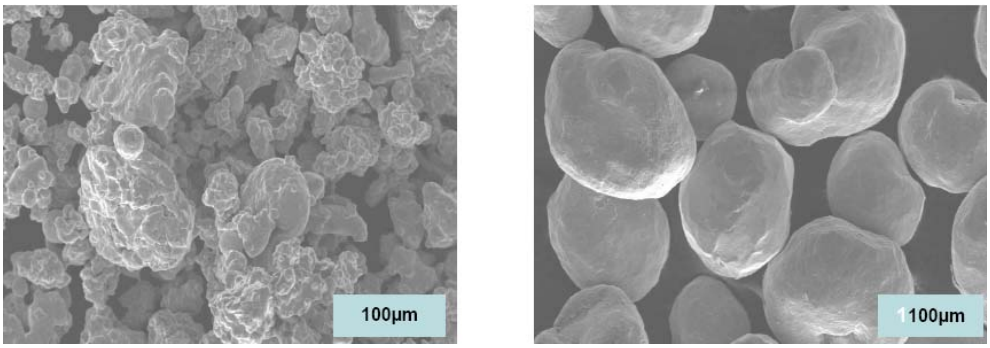

a) b)

Fig.1. Iron powder particle shape: a) as received, b) after milling.

Tab.1. Fe/SiO_2 powders prepared from two iron powders with different particle shape.

Coated Fe/SiO_2 powders		Iron powder		Calcination
Designation	Coating cont. [wt.%]	Particle size [μm]	Particle shape	
NPB	0.97	<200	irregular	at 400ºC for 3 hours in air
N1B	0.97	100-160		
N2B	0.98	45-63		
MPB	0.98	<160	spherical	
M1B	0.98	100-160		
M2B	0.99	45-63		
NPB+S	0.97	<200	irregular	
N1B+S	0.97	100-160		
N2B+S	0.98	45-63		
MPB+S	0.98	<160	spherical	
M1B+S	0.98	100-160		
M2B+S	0.99	45-63		

The Fe/SiO_2 powders were prepared by sol-gel method according to Yoldas [13], as follows: 50 g iron powder + 1.5 ml H_2O, 7g $Si(OR)_4$ and 50 ml C_2H_5OH were mixed in a magnetic stirrer for 60 min composite coated powders Fe/SiO_2 at 25ºC. Sol-gel coated powders were calcined at 400°C for 3 hours in air. Silane (3-glycidoxypropyltrimethoxysilane) was used as a binder added in an amount of 1.0 wt.%. Table1 summarizes the several experimental SiO_2 coated Fe composite powders prepared from iron powders of different particle shape and size. In all cases, the content of the

coating was 0.97-0.98 wt.%, which was achieved by carefully preparing the sol-gel coating with a high reproducibility; the deviation for the 10 coating experiments from the mean coating content was 0.49-1% for all the studied powders with different particle size and shape. The phase composition of the coating was analyzed by X-ray analysis. The apparent and tap densities were estimated (ISO 4490, ISO 3953) and the ratio tap density/apparent density was calculated (friction index).

Cylindrical specimens Ø10x5 mm^3 were cold pressed in a hard-metal die at uni-axial pressures from 50 to 800 MPa (3-5 specimens at each pressure); the density/porosity was determined by weighing and measuring the dimensions of the specimens with the accuracy of ± 0.0001 g and ± 0.005 mm. The compressibility of the powders was evaluated by the compression ratio (CR = ρ_{app}/ρ_{teor}), by relative density (RD = ρ/ρ_{teor}) and by porosity P (%) achieved at the pressing pressure "p". The compressibility was quantified using the compaction equation formulated by Parilák et al. [14]:

$$P = P_o \cdot \exp\left(-K \cdot p^n\right) \tag{1}$$

P_o (%) is the apparent porosity calculated from apparent density. Parameter K is related to powder particle morphology and parameter n is related to the ability of powder particles for densification by plastic deformation. The equation (1) enables one to calculate compressibility parameters that characterize the behaviour of metal powders during the compaction, as are:

Parameter "X_n" (for P → 0 at p → ∞):

$$X_n = \frac{P_0}{n}\left[\sqrt{2 \cdot \pi \cdot n} \Big/ \left(e \cdot \pi \cdot K\right)^{1/n}\right] \cdot \left[1 - \omega\left(1/n\right)\right], \text{ where } \omega\left(1/n\right) \leq e^{n/12} - 1 \tag{2}$$

which expresses the value of total „work" required for the densification of the compact to full density through a rearrangement (shift and rotation) and plastic deformation of the particles. Its value corresponds to the area under the compaction curve, until to P = 0.

Parameter "X_1" (for n = 1): $X_1 = P_0/K$ (3)

is that part of the "work" that is necessary for the densification of the compact through a rearrangement of particles (by shift and rotation) without plastic deformation development (for n = 1). It is a "fictitious" value, which corresponds to the area under the compaction curve defined by a fictitious porosity P_1. This assumption is an approximation, since the relocation of particles that have the ability to deform plastically, is always associated with a minimal plastic deformation of the surface roughness.

Pressure "p_1":

$$p_1 = \left[\ln\left(P_0\right) - \ln\left(P\right)\right] \cdot 1/K \tag{4}$$

which is a "fictitious" value of pressure (fictitious because it can only be obtained by calculation; a real one is not measurable) and reflects the pressure „p" needed for densification up to $P_1 = 0$. The value of the p_1 expresses the pressure at which is finished the densification dominantly by rearrangement (shift and rotation) and starts to dominate the densification by development of plastic deformation. At the pressure p_1 is reached a total porosity P_{p1}, which may be related to the state of geometric hardening of the powder system. Further densification with increasing pressure will take place by plastic deformation.

The microstructure of the compacts was studied by optical microscopy.

RESULTS AND DISCUSSION

Figures 2a,b show the metallographic section of the Fe/SiO_2 particles of the NPB and MPB powders. The coating is continuous with a thickness of 3000-5000 nm and has good cohesion with the surface of Fe particles. Defects were only sporadically identified; those such as cracking or inconsistencies, occurred especially in the case of irregularly shaped Fe particles. It should be noted that the coating on the surface of the Fe particle is also composed of Fe oxide phases that are modified by the heat treatment used. After calcination at 400ºC/air the layer consists of the phases: amorphous SiO_2, α-Fe_2O_3, Fe_3O_4 which have been predicted by ThermoCalc calculation and identified by X ray analysis, Fig.3, Fig.4. The ratio of the Fe-oxide was determined by chemical analysis of the Fe^{2+} and Fe^{3+} contents and up to ~ 30 wt.%.

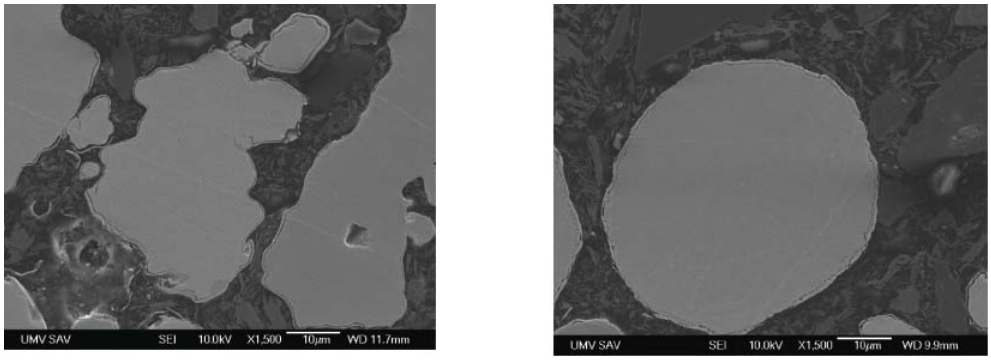

a) b)

Fig.2. Metallographic section of the Fe/SiO_2 coated particle a) with irregular shaped Fe particles (NPB), b) with spherical shaped Fe particles (MPB).

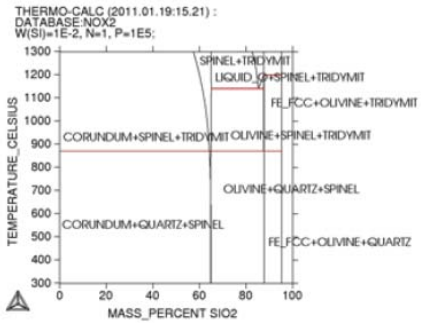

Fig.3. Theoretical phase diagram Fe_2O_3 -SiO_2, ThermoCalc Classic 4.0.

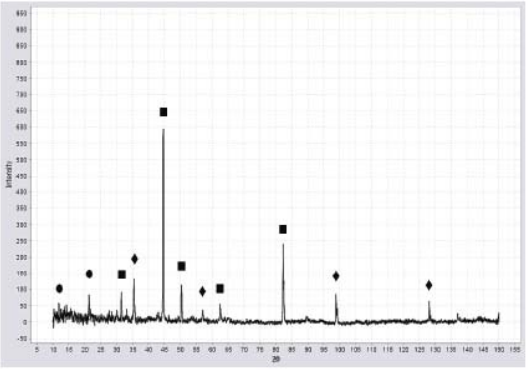

Fig.4. X-ray analysis of the coating calcined at 400°C (♦Fe_3O_4 ●SiO_2 ■ Fe_2O_3).

Table 3 summarizes the values of the theoretical density, apparent and tap densities, friction index and apparent porosity of the Fe/SiO_2 tested powders. It is visible that the apparent density of powders with irregular shaped Fe particles increases, while in the case of spherical particles there is the tendency for a slight decrease. A similar trend is also in the case of tap density. Silane addition leads to a slight increase of apparent density but slightly reduces the tap density which results in a slight decrease in friction index

values. Data summarized in Tables 4-6 show the relative density of the compacts in dependence on the compacting pressure. It is seen that the shape of Fe particles strongly influences the development of the relative density of compacts. As a result of higher apparent density the relative density is higher for the powders with spherical particle shape (48-55% when compared with 36-39% for irregular shape), particularly in the area of lower pressing pressures. The values of the relative density at a pressure of 800 MPa are in the range of 84-88%. The addition of Silane has a significant positive impact on the relative density, which, after pressing pressure 800 MPa reaches 93.5-96.5%. Figures 5a,b,c show the influence of both the shape and size of Fe particles and Silane addition to Fe/SiO_2 powders on the relative density of the compacts based on a) NP and MP powders, b) N1 and M1 powders, c) N2 and M2 powders. It can be seen that the joint effect of coating as well as the addition Silane was shown for powder based monodispersed Fe powders.

Tab.3. The basic physical properties of the Fe/SiO_2 powders.

Powder	ρ_{theor} [g/cm^3]	ρ_{app} [g/cm^3]	ρ_{tap} [g/cm^3]	Friction index	P_0 [%]
NP	7.845	2.965	3.733	1.252	62.205
NPB	7.783	3.107	3.982	1.281	60.080
NPB+S	7.245	2.999	3.572	1.193	58.577
N1	7.845	2.798	3.576	1.279	64.334
N1B	7.783	2.989	3.602	1.205	61.596
N1B+S	7.245	2.897	3.677	1.267	59.986
N2	7.845	2.811	3.677	1.306	64.145
N2B	7.783	2.823	3.553	1.258	63.729
N2B+S	7.243	2.925	3.902	1.339	59.669
MP	7.845	4.623	5.032	1.093	41.315
MPB	7.789	4.132	5.099	1.234	46.916
MPB+S	7.246	3.988	4.501	1.130	45.028
M1	7.845	4.147	4.840	1.169	47.138
M1B	7.783	4.108	4.762	1.159	47.218
M1B+S	7.245	4.333	5.072	1.174	40.193
M2	7.845	3.752	5.560	1.154	52.173
M2B	7.783	3.774	4.589	1.215	51.512
M2B+S	7.243	3.874	4.868	1.255	46.547

Tab.4. Relative density of compacts from NP, NPB, NPB+S, MP, MPB, MPB+S powders.

Pressure [MPa]	Relative density [%]					
	NP	NPB	NPB+S	MP	MPB	MPB+S
0	37.8	39.9	41.4	55.0	53.1	55.0
15	47.5	51.2	49.3	61.0	61.0	62.3
50	56.0	59.0	59.8	66.0	66.2	69.0
100	64.0	66.0	70.0	69.0	70.6	74.0
200	72.0	72.0	79.0	74.0	76.0	80.0
400	80.1	80.0	87.0	81.5	81.0	86.1
500	82.5	82.0	90.0	84.0	82.5	88.4
600	85.0	84.5	92.0	86.0	84.0	90.4
800	88.0	85.4	93.5	88.1	86.0	93.9

Tab.5. Relative density of compacts based on N1, N1B, N1B+S, M1, M1B, M1B+S powders.

Pressure [MPa]	Relative density. %					
	N1	N1B	N1B+S	M1	M1B	M1B+S
0	35.7	38.4	40.0	52.9	52.8	59.8
15	45.5	46.3	50.8	59.1	61.2	70.1
50	51.0	52.3	60.8	64.0	66.3	77.0
100	59.0	59.0	70.0	69.0	70.0	82.0
200	67.0	67.0	80.0	74.0	74.0	88.0
400	76.0	77.0	89.0	80.6	78.8	92.4
500	80.0	80.0	91.5	82.8	81.0	93.8
600	82.6	82.0	94.0	84.0	82.3	95.0
800	87.0	85.0	95.2	87.1	86.0	96.5

Tab.6. Relative density of compacts based on N2, N2B, N2B+S, M2, M2B, M2B+S powders.

Pressure [MPa]	Relative density. %					
	N2	N2B	N2B+S	M2	M2B	M2B+S
0	35.9	36.3	40.3	47.9	48.5	53.5
15	47.0	45.7	53.9	58.2	57.0	67.2
50	52.0	52.0	64.0	63.4	63.0	74.0
100	58.0	57.0	71.0	69.0	68.0	80.0
200	67.0	65.0	79.6	74.0	75.0	84.3
400	77.3	75.0	85.6	79.8	81.0	89.0
500	81.0	78.0	88.1	83.0	83.0	91.0
600	84.0	80.0	89.9	85.0	86.0	93.0
800	86.4	84.0	95.0	87.0	89.7	95.0

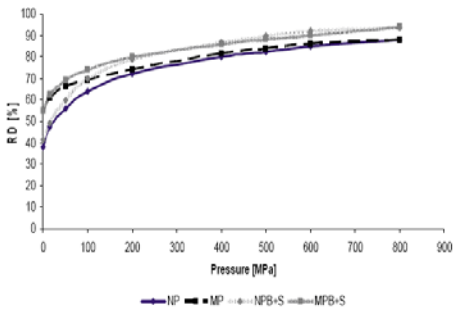

a)

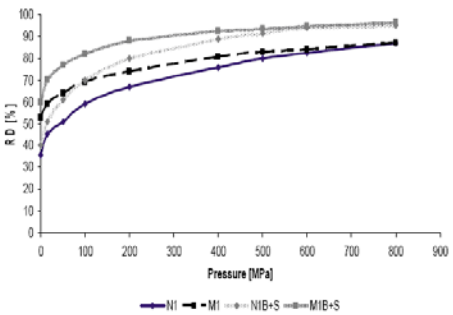

b)

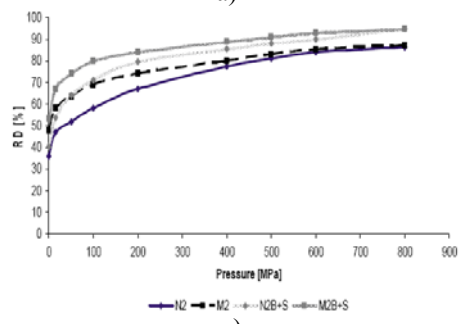

c)

Fig.5. The influence of both shape and size of Fe particles and Silane addition coated powder on relative density of the compacts based on (a) NP and MP powders, (b) N1 and M1 powders, (c) N2 and M2 powders.

In Tables 7-9 are the values of compression ratio for the tested powders. Lower values of the compression ratio of powders with spherical particles correspond to a higher apparent density. Silane addition slightly increases the compression ratio in the full compression pressure range. This effect is more pronounced in the case of a monodisperse of powders.

Tab.7. Compression ratio of the NP, NPB, NPB+S and MP, MPB, MPB+S powders.

Pressure [MPa]	Compression ratio					
	NP	NPB	NPB+S	MP	MPB	MPB+S
0	1.0	1.0	1.0	1.0	1.0	1.0
15	1.3	1.3	1.2	1.2	1.1	1.1
50	1.5	1.4	1.4	1.3	1.2	1.3
100	1.7	1.7	1.7	1.3	1.3	1.3
200	1.9	1.8	1.9	1.5	1.4	1.5
400	2.1	2.0	2.1	1.5	1.5	1.6
500	2.2	2.1	2.2	1.6	1.6	1.6
600	2.2	2.1	2.2	1.6	1.6	1.6
800	2.3	2.1	2.3	1.7	1.6	1.7

Tab.8. Compression ratio of the N1, N1B, N1B+S and M1, M1B, M1B+S powders.

Pressure [MPa]	Relative density [%]					
	N1	N1B	N1B+S	M1	M1B	M1B+S
0	1.0	1.0	1.0	1.0	1.0	1.0
15	1.3	1.2	1.3	1.1	1.2	1.2
50	1.4	1.4	1.5	1.2	1.3	1.3
100	1.7	1.5	1.7	1.3	1.3	1.4
200	1.9	1.7	2.0	1.4	1.4	1.5
400	2.1	2.0	2.2	1.5	1.5	1.5
500	2.2	2.1	2.3	1.6	1.5	1.6
600	2.3	2.1	2.3	1.6	1.6	1.6
800	2.4	2.2	2.4	1.6	1.6	1.6

Tab.9. Compression ratio of the N2, N2B, N2B+S and M2, M2B, M2B+S powders.

Pressure [MPa]	Compression ratio					
	N2	N2B	N2B+S	M2	M2B	M2B+S
0	1.0	1.0	1.0	1.0	1.0	1.0
15	1.3	1.3	1.3	1.2	1.2	1.3
50	1.5	1.4	1.6	1.3	1.3	1.4
100	1.6	1.6	1.8	1.4	1.4	1.5
200	1.9	1.8	2.0	1.5	1.5	1.6
400	2.2	2.1	2.1	1.7	1.7	1.7
500	2.3	2.2	2.2	1.7	1.7	1.7
600	2.3	2.2	2.2	1.8	1.8	1.7
800	2.4	2.3	2.4	1.8	1.9	1.8

Figures 6a-c display the compaction curves for the coated powders with irregular and spherical particles. Figures 7a-c show the compaction curves for the same powders

with the addition of a Silane binder. The traces in the diagrams are the representation of the compaction equations (1) and (4) which quantify the compressibility of the powders; the correlation coefficients obtained by fitting the experimental data with equation (1) are in the range of 0.967-0.9982 which means that the equation (1) can be also considered as applicable for the coated powders studied. The values of the compaction parameters p_1, P_{p1}, X_n, X_1, $P_{800,}$ whose meaning was given in the experimental section, are in Table 10.

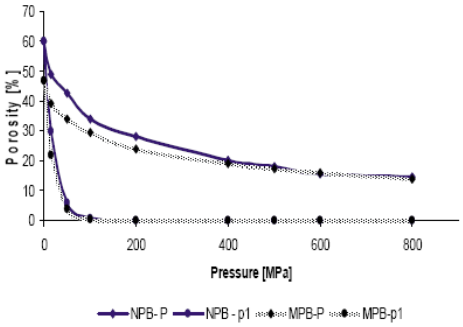

Fig.6a. Compaction curves for NPB, MPB powders:
NPB 60.09 exp(-0.047·p $^{0.5284}$); r = 0.9704
MPB 46.91 exp(-0.051·p $^{0.5057}$); r = 0.9982
NP 62.21 exp(-0.0367·p $^{0.5818}$); r = 0.9859

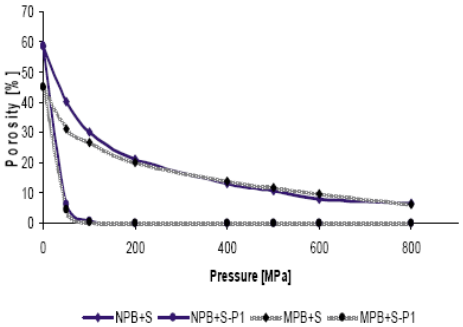

Fig.7a. Compaction curves for NPB+S, MPB+S powders:
NPB+S 58.58 exp(-0.035·p $^{0.6509}$); r = 0.9567
MPB+S 45.03 exp(-0.034·p $^{0.6047}$); r = 0.9849
MP 43.13 exp(-0.0283·p $^{0.5889}$); r = 0.9738

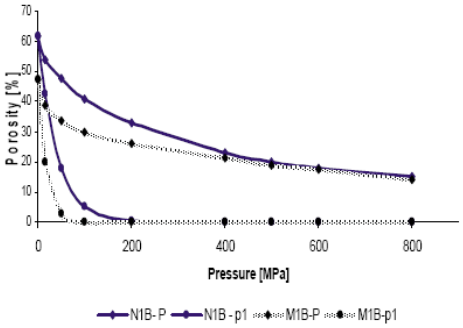

Fig.6b. Compaction curves for N1B,. M1B powders:
N1B 61.569 exp(-0.026·p $^{0.6195}$); r = 0.9759
M1B 47.218 exp(-0.057·p $^{0.5025}$); r = 0.9884
N1 64.334 exp(-0.032·p $^{0.5796}$); r = 0.9888

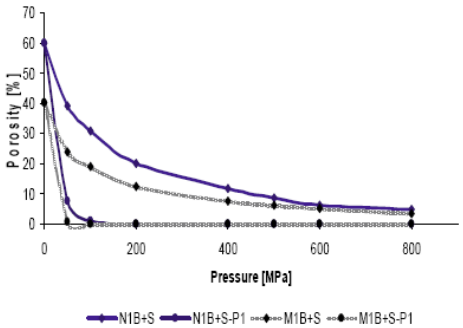

Fig.7b. Compaction curves for N1B+S, M1B+S powders:
N1B+S 59.986 exp(-0.0324·p $^{0.6693}$); r = 0.9665
M1B+S 40.193 exp(-0.0679·p $^{0.5435}$); r = 0.9775
M1 45.030 exp(-0.0296·p $^{0.5743}$); r = 0.9651

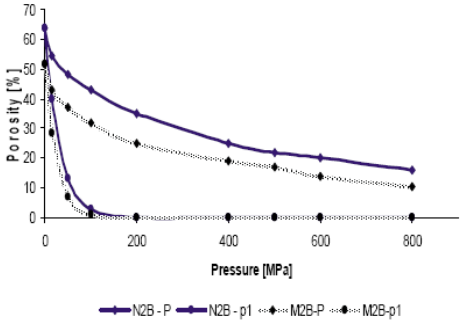

Fig.6c. Compaction curves for N2B, M2B powders:
N2B 63.729 exp(-0.0314·p $^{0.5726}$); r = 0.9683
M2B 51.519 exp(-0.0386·p $^{0.5680}$); r = 0.9932
N2 64.145 exp(-0.0182·p $^{0.6830}$); r = 0.9624

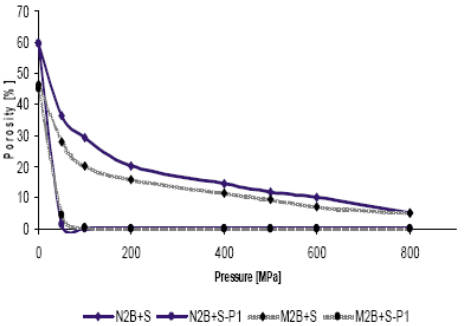

Fig.7c. Compaction curves for N2B+S, M2B+S powders:
N2B+S 59.669 exp(-0.0576·p $^{0.5532}$); r = 0.9781
M2B+S 46.547 exp(-0.0898·p $^{0.5011}$); r = 0.9902
M1 52.147 exp(-0.0501·p $^{0.5050}$); r = 0.9789

Tab.10. Values of the compaction parameters p_1, P_{p1}, X_n, X_1, P_{800}.

Powder	Type	P_0 [%]	p_1 [MPa]	P_{p1} [%]	X_1	X_n	P_{800} [%]*
NP	uncoated	62.205	238	25.6	17	296	12.0
MP		43.133	297	20.6	16	303	10.1
NPB	coated	60.088	186	28.9	13	374	14.6
MPB		46.912	165	24.3	10	372	13.4
N1	uncoated	64.334	287	28.3	20	374	12.9
M1		45.030	285	22.0	16	330	11.8
N1B	coated	61.569	355	24.2	25	328	17.0
M1B		47.218	148	23.6	8	281	14.7
N2	uncoated	64.145	481	18.6	35	258	13.6
M2		52.147	171	26.6	10	371	12.6
N2B	coated	63.729	279	29.0	20	410	15.9
M2B		51.519	222	23.6	13	284	10.2
NPB+S	coated + 1.0 wt.% Silane	58.577	266	17.1	18	137	6.4
MPB+S		45.028	242	17.0	13	161	6.0
N1B+S		59.986	268	15.2	18	114	4.0
M1B+S		40.193	122	15.9	6	92	5.0
N2B+S		59.669	150	23.0	10	164	5.0
M2B+S		46.547	94	19.0	5	108	5.0

* P_{800} means the porosity achieved at the pressing pressure of 800 MPa.

There is a clear difference between the compaction curves for powders NPB and MPB. Figure 6a with irregular and spherical particles at low pressures which corresponds to the densification by rearrangement of particles (shift and rotation). It is obvious that a denser arrangement of spherical particles already in the „free-pouring" state heavily restricts the processes of particle rearrangement. However, the friction between the particles is also acting; the surface roughness causes that, while the values of the pressure p_1 (Tab.10) are about the same, the values of porosity P_{p1} at p_1 and of the work (X_1) needed for

densification by rearrangement of particles are lower for the spherical particles. The value of the „work" X_n needed for densification by plastic deformation is comparable for both powders. Comparing the values of X_n with those of the same uncoated powders (NP, MP, Tab.10) shows that the values are lower for uncoated powders. This reflects the negative influence of coating on powder densification by plastic deformation which results in the slightly higher porosity reached at p = 800 MPa for the coated powders, while the particle shape does not have significant effect on compressibility behaviour.

The addition of Silane to both powders (NPB+S and MPB+S), Fig.7a, increases the value of p_1 but decreases the value of P_{P1} which means that Silane has a positive effect on the densification in the stage of rearrangement of particles by shift and rotation. A more dense arrangement of the particles enables a more effective development of plastic deformation resulting in a significant decrease of porosity, up to 6-6.4% for p = 800 MPa (Tab.10).

The difference between the compaction behaviour of irregular and spherical particles is also observed in the case of monodisperse powders N1B and M1B (Fig.6b). Thus the pressure p_1 and the values of P_{P1} are significantly higher for powders with irregular particles than with spherical particles (Tab.10). Data in Tab.10 show that the parameter X_1 is much smaller for powders with spherical particles than for those with irregular particles. For pressures higher than p_1 the compaction curves are similar for both powders - the densification is controlled by the ability of the iron core to deform plastically. The porosity achieved for p = 800 MPa is lower for the powder with spherical particles. As for the polydisperse powders (NPB, MPB), the addition of a Silane binder, Fig.7b, has a positive effect on particle rearrangement (lower value of X_1. Tab.10). Following a denser arrangement of particles, the plastic deformation of iron particles is more effective and the densification is greater which results in lower porosity of 4.8-5.0% for p = 800 MPa.

The monodisperse coated powders with fine particles (N2B, M2B), Fig.6c, showed a compaction behaviour comparable to the powders N1B and M1B. Comparing the M1B and M2B powders (Tab.10) with spherical particles of a different size, the pressure p_1 is shifted to a higher value for finer particles, practically at the same value of P_{p1} but at higher X_1 value; the resulting porosity for p = 800 MPa is lower for the powder M2B with fine spherical particles (10.2%) than for M1B (14.7%). The addition of Silane (Fig.7c) reduces the value X_1, mainly for spherical particles. Due to a denser arrangement of particles and thus a more effective development of plastic deformation (lower X_n values), the addition of Silane leads to a lower porosity of 5% for p=800 MPa, for both powders with irregular and spherical particles when compared with powders without the Silane addition.

Figures 8a,b and 9a,b show examples of the microstructure of compacts based on the powders N1B+S and M1B+S pressed at the pressures of 400 and 800 MPa. It is seen that the coating forms a continuous network without microscopically obvious cracks or other damage even when using a high compacting pressure. The continuous network in the compact shows a good bond of the coating with the iron particle, even when handling the powder and during compaction as well. The morphology of the network is determined by the shape of the deformed iron powder particles.

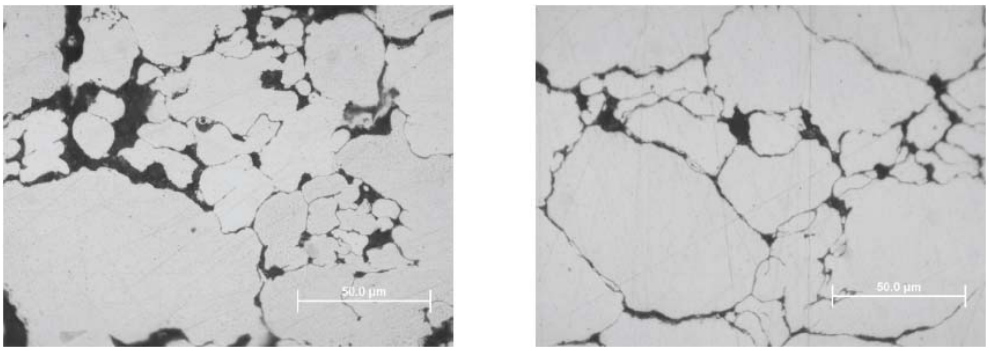

a) b)

Fig.8. The microstructure of the compact based on the Fe/SiO_2 powder with irregular shaped Fe particles and with addition of Silane (N1B+S), compacted at (a) 400 MPa, (b) 800 MPa.

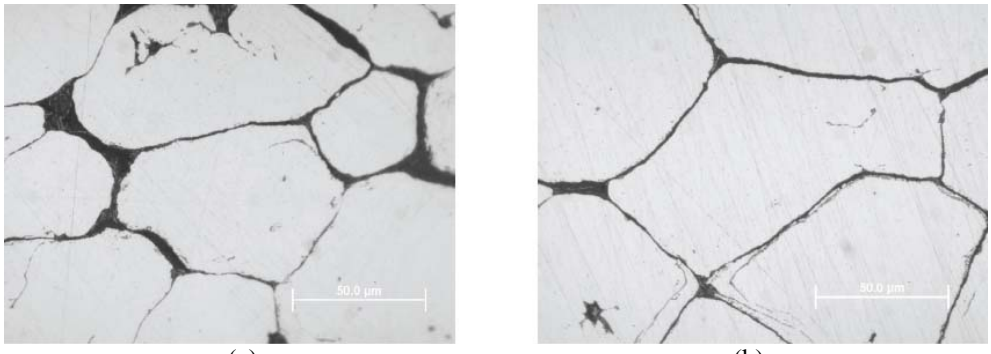

(a) (b)

Fig.9. The microstructure of the compact based on the Fe/SiO_2 powder with spherical Fe particles and with addition of Silane (M1B+S), compacted at (a) 400 MPa, (b) 800 MPa.

The microstructure of the compacts resulting from the pressure of 400 MPa is comprised of residual pores; also some local plastic deformation can be identified, particularly in areas of particle contacts. The compaction at the pressure of 800 MPa, which corresponds to the relative density of 95% for both presented powders results in a disappearance of large pores that are filled with surface roughness and fine particles. The densification process is supported by the positive effect of Silane, as well as by localized plastic deformation and intensive volume plastic deformation of Fe particles. The insulating coating follows well the surface of deformed particles.

CONCLUSIONS

The coating has a slightly negative effect on the compressibility, which is reflected in the slightly higher values of the porosity after compaction at a pressing pressure of 800 MPa when compared with the same uncoated powders.

After exhausting the possibilities of rearrangement of particles by shift and rotation (geometrical hardening state), the densification is further controlled by plastic deformation of the iron core inside the composite particles.

The differences between the compressibility of powders with irregular and spherical particles were identified in the area of low pressures which corresponds to the densification through particle rearrangement (shift and rotation). A denser arrangement of spherical particles, already in the loose state, heavily restricted the relocation processes.

The addition of 1.0 wt.% Silane binder to the coated powders with irregular and spherical particles has a significantly positive effect on compressibility. The decrease of porosity after compaction at the pressing pressure 800 MPa is two to three-folds when compared to the same coated powders without the binder addition.

Acknowledgements

The contribution was prepared within the framework of grant APVV LPP-0246-07. The authors wish to thank the Slovak Agency APVV Slovak National Grant Agency for its financial support.

REFERENCES

[1] Rosso, M.: Journal of Materials Processing Technology, vol. 175, 2006, p. 364
[2] Yan, CZ., Shi, YS., Yang, JS., Liu, JH.: Journal of Materials Processing Technology, vol. 209, 2009, no. 17, p. 5785
[3] Narasimhan, K., Hanejko, F., Marucci, ML. In: EURO PM 2007, vol. 1, p. 325
[4] Capus, JM.: Metal Powder Report, 2002, January, p. 20
[5] Andersson, O., Hofecker, P. In: Powder Met., 2009. Las Vegas, USA, July, 2009, p. 1
[6] Hultman, L., Andersson, O. In: EURO PM2009. Copenhagen, October 13, 2009, p. 1
[7] Uozumil, G., Watanabe, M., Nakanabe, R., Kazunori, I.: Materials Science Forum, vols. 534-536, 2007, p. 1361
[8] Taghvaei, AH., Ebrahimi, A., Ghaffari, M., Janghorban, K.: Journal of Magnetism and Magnetic Materials, vol. 322, 2010, p. 808
[9] Yang, B., Zhangben, W., Zhiyu, Z., Ronghai, Y.: J. Appl. Phys., vol. 43, 2010, 365003
[10] Somaloy® Technology for Electric Motors. Höganäs AB, Sweden, March 2011
[11] Somaloy® Technology for Power Electronics. Höganäs AB, Sweden, March 2011
[12] Katsuhiko, M., Masahisa, M., Koichiro, M., Kazunori, I.,. Muneako, W., Nakayama, R. In: Powder Met., 2008. Vol. 10. Washington, USA, p. 261
[13] Yoldas, BE., Partlow, DP.: Thin Solid Films, vol. 129, 1985, p. 1
[14] Parilák, Ľ., Dudrová, E., Bidulský, R., Kabátová, M. In: EURO PM 2004. Vol. 1. Vienna, 2004. EPMA, 2004, p. 593